Raman-scattering spectra of coupled LO-phonon–hole-plasmon modes in *p*-type GaAs

R. Fukasawa and S. Perkowitz
Department of Physics, Emory University, Atlanta, Georgia 30322-2430
(Received 1 June 1994; revised manuscript received 25 July 1994)

We have measured the room-temperature Raman spectra of the coupled LO-phonon–damped-hole-plasmon modes of ten *p*-type, Be-doped, molecular-beam-epitaxy-grown GaAs films with hole concentrations from 6.3×10^{17} to 2.9×10^{19} cm^{-3}. Although coupled-mode theory predicts the existence of two modes, we observed only one, with an asymmetric line shape. A line-shape analysis combining the deformation-potential and electro-optic mechanisms shows that the theory reproduces the data very well. It also suggests that one mode is suppressed by the large damping of the hole plasmon. The asymmetry of the observed peak is shown to come from interference between Raman scattering from atomic displacement fluctuations and that from macroscopic electric-field fluctuations. The ratio between Hall mobilities of the holes and optical mobilities of the holes from the Raman measurements is $\mu_{\rm Hall}/\mu_{\rm optical}=1.5$–$2.6$ for different hole concentrations.

I. INTRODUCTION

In a polar semiconductor, the plasmon formed by the free carriers and a longitudinal-optical (LO) phonon interact via their macroscopic electric fields.[1,2] The coupled LO-phonon–plasmon (LO-PL) modes from such interactions have been extensively studied in *n*-type semiconductors such as *n*-type GaAs by Raman spectroscopy[3] and far-infrared spectroscopy.[4] However, there have been few studies of the coupled modes in doped *p*-type direct-gap compound semiconductors. Our first motivation in this work is to explore the fundamental properties of the coupled modes in a *p*-type material with the use of Raman spectroscopy. A second motivation is to study the coupled modes under conditions of high plasmon damping. This investigation of the dynamical response of the phonon and hole systems also provides a way to optically characterize carrier concentrations and mobilities of *p*-type material.

In earlier work,[5] one of the present authors (R.F.) and co-workers measured the Raman spectra of six Be-doped *p*-type molecular-beam-epitaxy- (MBE) grown GaAs samples. Furthermore, Fukasawa *et al.*[6] have analyzed semiquantitatively the Raman spectra[5] from four *p*-type GaAs samples with a theory of Raman scattering that included surface depletion effects in a doped opaque semiconductor. They concluded that a broad band near the transverse-optical (TO) phonon frequency $\omega_{\rm TO}$ represents the lower branch of the coupled LO-PL modes and suggested that the lower branch is phononlike while the overdamped upper branch is not observable.

Other measurements show a variety of results. Yuasa and Ishii[7] have reported Raman spectra from the (100) surface of Be-doped *p*-type GaAs grown by MBE with hole concentrations from 1×10^{16} to 2×10^{19} cm^{-3}. They observed the upper branch of the LO-PL modes on the high-frequency side of the LO-phonon frequency $\omega_{\rm LO}$ for $p=3\times10^{18}$ cm^{-3} and found the lower branch of the coupled modes near $\omega_{\rm TO}$ for $p=2\times10^{19}$ cm^{-3}. Their spectra resembled some of ours, but they did not make measurements at the most critical values of hole concentrations. Without these data, they concluded that the coupled LO-phonon–hole-plasmon modes in *p*-type GaAs are like those in *n*-type material, an interpretation that other measurements and our analysis do not support.

More recently Wan *et al.*[8,9] have reported Raman spectra from the (100) surface of Be-doped, MBE-grown, *p*-type GaAs with hole concentrations of $p=1\times10^{18}$ to 3×10^{19} cm^{-3}. They observed only a single coupled mode at a frequency between the LO- and TO-phonon frequencies for hole densities between 1×10^{18} and 1.6×10^{19} cm^{-3}. They pointed out that the coupled modes in *p*-type GaAs do not behave like those seen in *n*-type GaAs.

These disagreements about the behavior of the coupled modes as a function of hole concentration may come from the limited experimental data and the difficulty of analyzing a complex Raman profile that combines the LO-phonon–damped-hole-plasmon modes in the bulk and the "unscreened" LO phonon in a surface depletion layer. To fully examine this situation in *p*-type GaAs, we have performed Raman scattering experiments on ten Be-doped *p*-type GaAs samples over a wide range of hole concentrations. We added four samples to the suite we measured earlier[5] to extract systematic trends as a function of hole concentration. We observed only one mode of an asymmetric nature at all hole concentrations. We analyze the complex Raman profile by applying the theory of first-order phonon Raman scattering from an opaque semiconductor derived by Katayama and Murase[10] and Fukasawa *et al.*[6] These calculations assume that the electronic susceptibility is modulated by the atomic displacement field (deformation-potential mechanism) and the macroscopic electric field (electro-optic mechanism).[11]

The contribution to the Raman efficiency of the coupled modes from the electro-optic mechanism is negligibly small under the condition of large plasmon damping, which means that the coupled modes in *p*-type GaAs are

phononlike. The hole-plasmon-damping constant and optical mobility μ_{op} are determined from the line-shape analysis and compared with the Hall mobilities μ_H. We obtained the ratio $\mu_H/\mu_{op}=1.5-2.6$ for different hole concentrations.

II. EXPERIMENT

Ten Be-doped p-type GaAs epitaxial films with hole concentrations ranging from 6.3×10^{17} to 2.9×10^{19} cm^{-3} were grown on (100) semi-insulating GaAs substrates by molecular-beam epitaxy, using a computer-controlled Riber machine at the Electrotechnical Laboratory, Japan.[12] The films were about 1.2 μm thick. The hole concentrations and mobilities were determined from Hall measurements at room temperature. Characteristics of the samples are given in Table II.

Unpolarized Raman measurements were performed in the near-backscattering geometry at room temperature, using the 5145-Å(2.41-eV) line of an Ar^+-ion laser with a power of about 400 mW. The optical penetration depth of the incident light is ~0.1 μm, much less than the thickness of the film. The scattered light from an illuminated spot ~300 μm in diameter on the sample surface was collected in a direction near normal to the surface and focused by an $f/1.2$ camera lens on the entrance slit of a SPEX triplemate spectrograph equipped with a subtractive stage containing two gratings, and a dispersive stage containing a 2400-lines/mm holographic grating. A sensitive optical multichannel analyzer detected the scattered light. Each data set consisted of 30 spectra, exposed for 1 min each. The entrance slit, intermediate slit, and entrance slit of the dispersive stage were set at 0.1, 4, and 0.05 mm, respectively. The wave-number scale of the spectrograph was calibrated by using the known Raman lines of toluene. The accuracy of the Raman shift was ±0.5 cm^{-1}. The spectral resolution of our spectrograph was 1.3 cm^{-1}.

III. RESULTS AND DISCUSSION

Figure 1 shows the Raman spectra of the ten samples. The unscreened LO-phonon line appears at 290 cm^{-1} for all hole concentrations. A broad band is seen near the TO-phonon frequency (267 cm^{-1}) in samples (g)–(j) with hole concentrations $\geq1.5\times10^{19}$ cm^{-3}. Shoulders at the high- and low-frequency sides of the unscreened LO-phonon line are seen for samples (e) and (f), whereas only a high-frequency shoulder is seen for samples (a)–(d). The full widths at half maximum (FWHM) of the unscreened LO-phonon line for samples (a), (b), (c), and (d) are 7, 9, 13, and 14.5 cm^{-1}, respectively, all much larger than the FWHM of 4.4 cm^{-1} for semi-insulating GaAs. This may be due to the superposition of two nearby Raman bands, one from the unscreened LO-phonon mode, one from the coupled LO-PL modes. Raman scattering by the TO-phonon mode is forbidden for a true backscattering geometry for a (100) surface of a zinc-blende crystal.[13] However, a weak TO-phonon line is observed at 266.5 cm^{-1} in samples (a)–(c) because the incident light is not exactly normal to the surface of the sample.

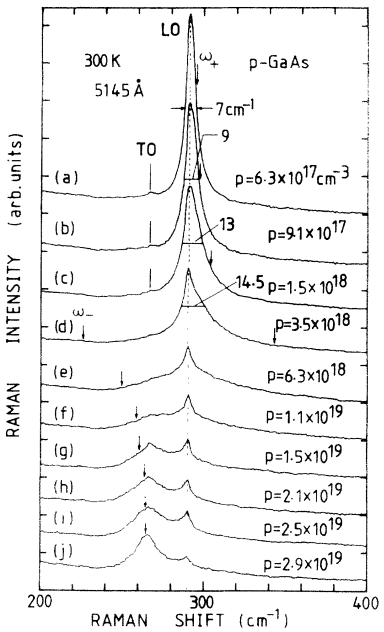

FIG. 1. Raman spectra from the ten Be-doped p-type GaAs samples listed in Table II. All spectra were obtained in the backscattering geometry at room temperature, using the 5145-Å line of the Ar^+-ion laser. The arrows denoted ω_+ and ω_- are the frequencies predicted by the coupled mode theory. The full widths at half maximum of the Raman spectra are 7, 9, 13, and 14.5 cm^{-1} for samples (a), (b), (c), and (d), respectively.

According to the coupled-mode theory, the frequencies of two coupled LO-PL modes in a doped polar semiconductor in the limit of long wavelength, and with no phonon or plasmon damping, are given by[1,2]

$$\omega_\pm^2=\tfrac{1}{2}\{(\omega_{LO}^2+\omega_p^2)\pm[(\omega_{LO}^2+\omega_p^2)^2-4\omega_p^2\omega_{TO}^2]^{1/2}\}\ , \qquad (1)$$

where ω_p is the hole plasma frequency defined by $\omega_p^2=4\pi pe^2/\epsilon_\infty m_h^*$. ϵ_∞, p, and m_h^* are the optical dielectric constant, the hole concentration, and the effective mass of the free hole, respectively. Figure 2 shows the calculated frequencies (ω_- and ω_+) of the coupled LO-PL modes in p-type GaAs plotted as a function of hole concentration. The material parameters for GaAs used in the calculation are listed in Table I. The effective mass of free hole in p-type GaAs was estimated by considering the degeneracy at $k=0$ of the light-hole and heavy-hole bands. Following the well-known two-band transport theory,[14,15] the average hole effective mass is estimated to be $m_h^*=0.34m$ with the light- and heavy-hole masses 0.09 and $0.45m$,[16] respectively.

For samples (a)–(c) (see Fig. 1), the shoulder extending to the high-frequency side of the unscreened LO-phonon line is seen near the upper-mode frequency ω_+ calculated from Eq. (1). These shoulders come from the upper branch of the coupled LO-PL modes. However, no upper branch of the coupled modes is seen at the upper-mode frequency ω_+ for samples (d)–(j) with hole concentrations ($p\geq3.5\times10^{18}$ cm^{-3}). On the other hand, the peak of the lower branch is not seen at the lower-mode fre-

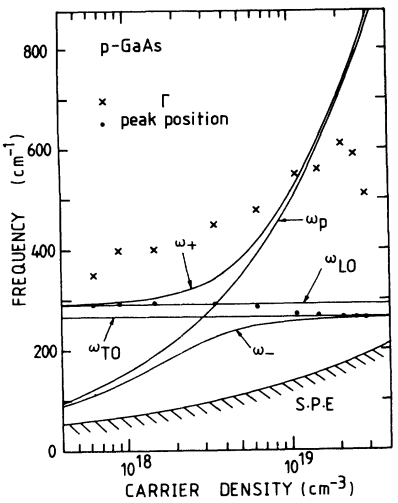

FIG. 2. The predicted frequencies of the coupled modes (ω_+ and ω_-) and the plasmon mode ω_p as a function of the carrier densities. ω_{LO} and ω_{TO} are the LO- and TO-phonon frequencies. The hatched area expresses the regime of single-particle excitations (SPE) bounded by $\omega(q)=qv_F+\hbar q^2/2m_h^*$, where v_F is the Fermi velocity. The wave vector q was taken as listed in Table I. The closed circles show the spectral peak positions of the fitted spectra drawn by the broken lines in Fig. 3. The symbol × shows the plasmon damping constant obtained from the fitting.

quency ω_- for samples (a)–(h). These spectral features of p-type GaAs specimens are quite different from the spectra of n-type GaAs reported in earlier papers.[3]

To explore the dependence on hole concentration of Raman spectra of p-type GaAs, we performed a line-shape analysis combining the deformation potential and electro-optic mechanisms for an opaque semiconductor,[6,10] the dominant mechanisms for unpolarized scattering under nonresonant conditions.[17]

As derived by Katayama and Murase,[10] the Raman line-shape function g_T is

$$g_T=g_1+g_2+g_3 , \tag{2}$$

TABLE I. Material parameters of p-type GaAs.

ω_{LO}	LO-phonon frequency	290.0 cm^{-1}
ω_{TO}	TO-phonon frequency	266.5 cm^{-1}
ϵ_∞	Optical dielectric constant	10.9[a]
ϵ_0	Static dielectric constant	12.9[a]
C	Faust-Henry coefficient	−0.59[b]
m_h^*	Average hole effective mass	0.34 m
v	Constant of velocity	4.73×10^5 cm/s[c]
q	Scattering wave vector	1.05×10^6 cm^{-1}[d]
α	Absorption coefficient	0.833×10^5 cm^{-1}[d]
ϕ	Barrier height	0.5 eV[e]

[a]Data from Ref. 24.
[b]Data from Ref. 25.
[c]Data from Ref. 22.
[d]Data from Ref. 10.
[e]Data from Ref. 26.

$$g_1=\frac{C^2\omega_{TO}^4}{(\omega_{LO}^2-\omega_{TO}^2)^2}\hbar[n(\omega)+1]\times\mathrm{Im}[(4\pi)^2\chi_{ph}(\epsilon_\infty+4\pi\chi_{fc})/\epsilon_\infty^2\epsilon] , \tag{3}$$

$$g_2=-\frac{2C\omega_{TO}^2}{\omega_{LO}^2-\omega_{TO}^2}\hbar[n(\omega)+1]\mathrm{Im}[(4\pi)^2\chi_{ph}/\epsilon_\infty\epsilon] , \tag{4}$$

$$g_3=\hbar[n(\omega)+1]\mathrm{Im}[-4\pi/\epsilon] , \tag{5}$$

where C is the Faust-Henry coefficient,[18] $n(\omega)$ is the Bose-Einstein factor, and the total dielectric function ϵ for the phonon and free-carrier system is given by

$$\epsilon=\epsilon_\infty+4\pi\chi_{ph}+4\pi\chi_{fc} , \tag{6}$$

$$4\pi\chi_{ph}=\epsilon_\infty\frac{\omega_{LO}^2-\omega_{TO}^2}{\omega_{TO}^2-\omega^2-i\omega\gamma} , \tag{7}$$

$$4\pi\chi_{fc}=-\epsilon_\infty\frac{\omega_p^2}{\omega(\omega+i\Gamma)} , \tag{8}$$

where χ_{ph}, χ_{fc}, γ, and Γ are the ionic susceptibility, the free-carrier susceptibility, the phonon damping constant, and the plasmon damping constant, respectively. In Eq. (2), g_1 arises from the fact that the first-order Raman susceptibility is modulated by the atomic displacement. g_3 arises from the fact that the Raman susceptibility is modulated by the macroscopic electric field associated with the coupled modes. g_2 is the cross correlation term between the atomic displacement and the macroscopic electric field.[10,11]

To calculate the line shape, we need the material parameters p, ω_{LO}, ω_{TO}, ϵ_∞, C, m_h^*, Γ, and γ, respectively. The values of ω_{LO}, ω_{TO}, ϵ_∞, C, and m_h^* for GaAs listed in Table I were fixed for all calculations. The hole concentrations p are given in Table II for each sample. Taking γ and Γ as adjustable parameters, we fitted the spectra in the best least-squares fit sense, except that the peak near 290 cm^{-1} was separately fitted with an optimized Lorentzian function. The results are shown in Fig. 3. Table II shows the values of γ and Γ obtained from the fitting. For samples (d)–(f), the calculation reproduces observed asymmetric broadbands with a tail extending to the high-frequency side of the unscreened LO-phonon line and the broad feature at about 265 cm^{-1} in samples (g)–(j). But the calculated spectra do not reproduce the unscreened LO-phonon line from the surface depletion layer. The frequencies of the coupled LO-PL modes denoted by ω_+ and ω_- in Fig. 3 were obtained from Eq. (1). The closed circles in Fig. 2 show the spectral peak positions of the calculated spectra (broken lines) in Fig. 3. The behavior of the peak positions with hole concentration is similar to the result shown in Fig. 4 of Ref. 9 obtained by Wan and Young. The peak positions of the coupled modes in p-type GaAs do not correspond to the frequencies predicted from Eq. (1) as shown in Fig. 2, whereas Eq. (1) does give the correct coupled-mode frequencies for n-type GaAs.[3] The crosses in Fig. 2 represent the plasmon damping constant Γ obtained from the line-shape analysis. ω_p is larger than Γ for samples with higher hole concentrations ($p\geq1.5\times10^{19}$ cm^{-3}), a

TABLE II. Parameters for the ten Be-doped p-type GaAs samples. The hole concentration p and mobility μ_H are determined by Hall measurements. The thickness of surface depletion layer d_L is estimated by using the Schottky barrier model. The phonon damping constant γ, the hole-plasmon damping constant Γ, the phonon damping constant of the unscreened LO phonon γ_1, the peak frequency ω_R of the single coupled mode, and the optical mobility μ_{op} are determined by Raman measurements.

Sample	p (cm^{-3})	μ_H ($cm^2/V\,s$)	d_L (Å)	γ (cm^{-1})	Γ (cm^{-1})	γ_1 (cm^{-1})	ω_R (cm^{-1})	μ_{op} ($cm^2/V\,s$)
(a)	6.3×10^{17}	190	336	4.4	350	5.0	291.5	78
(b)	9.1×10^{17}	177	280	4.8	400	6.7	292.0	69
(c)	1.5×10^{18}	158	218	5.0	400	7.0	293.0	69
(d)	3.5×10^{18}	128	143	5.0	450	7.0	293.5	61
(e)	6.3×10^{18}	118	106	5.8	480	7.5	285.5	57
(f)	1.1×10^{19}	85	81	6.0	550	7.5	273.0	50
(g)	1.5×10^{19}	72	69	6.2	560	8.0	269.0	49
(h)	2.1×10^{19}	69	58	6.5	610	8.0	267.0	45
(i)	2.5×10^{19}	76	53	7.0	590	8.0	266.5	47
(j)	2.9×10^{19}	82	50	6.2	510	9.0	265.5	54

condition of relatively light damping for the hole plasmon. On the other hand, ω_p is smaller than Γ for samples with lower hole concentrations ($p \leq 1.1\times10^{19}$ cm^{-3}), a condition of heavier damping.

Figure 4 compares the mobilities μ_H obtained from Hall measurements to values obtained from the line-shape analysis using $\mu_{op}=e/m_h^*\Gamma$. The ratio μ_H/μ_{op} is 1.5 to 2.6 for different hole concentrations. Similar differences have been reported in p-type GaAs. Gargouri, Prevot, and Schwab[19] made Raman measurements in Be-implanted p-type GaAs and obtained $\mu_H/\mu_{op}=3.7$. More recently Mlayah *et al.*[20] obtained $\mu_H/\mu_{op}\sim2$ from Raman measurements in Be-doped p-type GaAs. They speculated that the difference may come from the fact that the mobilities are measured at different frequencies, but we are aware of no detailed argument that explains why $\mu_H\neq\mu_{op}$. However, since ω_- and ω_+ are not in the regime of single-particle excitation (see Fig. 2), it is clear that the coupled modes are unaffected by Landau damping.[3]

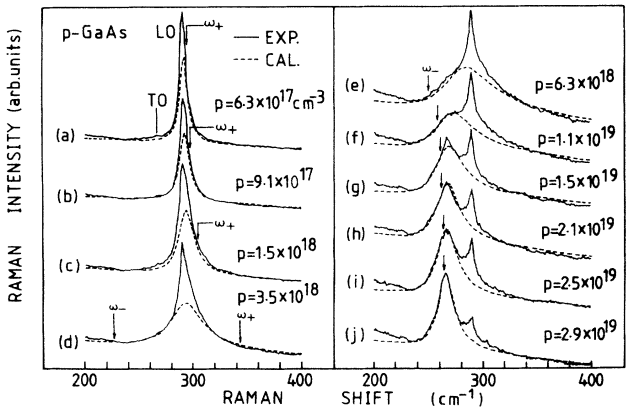

FIG. 3. Experimental (solid lines) and theoretical (broken lines) Raman spectra of the ten p-type GaAs samples. The arrows denoted ω_+ and ω_- are the predicted frequencies by the coupled-mode theory.

We further analyzed the Raman spectra to determine the cause of the asymmetric line shape. Figure 5 shows the results of Fig. 3 broken down into the separate terms g_1, g_2, and g_3 in Eqs. (3)–(5). g_1 and g_3 arise from atomic displacement fluctuations and macroscopic electric field fluctuations, respectively. The term g_2 comes from interference between the two kinds of fluctuations.[10] The contribution of g_3 is negligible at all hole concentrations and the calculated spectrum is the superposition of g_1 and g_2. At low concentrations ($p \leq 1.5\times10^{18}$ cm^{-3}), g_1 and g_2 are of comparable size and give a symmetric peak. The theoretical spectra begin to become asymmetric for $p \geq 3.5\times10^{18}$ cm^{-3}, where g_2 becomes asymmetric.

Figure 6 demonstrates the effect of plasmon damping on line shape by assuming four different values of Γ at $p=6.3\times10^{18}$ cm^{-3}, where $\omega_p=391$ cm^{-1}, $\omega_-=249$

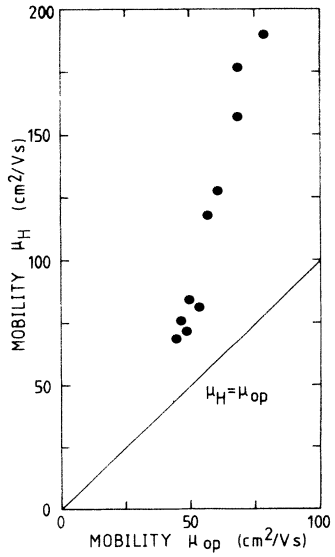

FIG. 4. The optical mobilities μ_{op} obtained from the Raman measurements compared with results of Hall measurements. The solid line represents $\mu_H=\mu_{op}$.

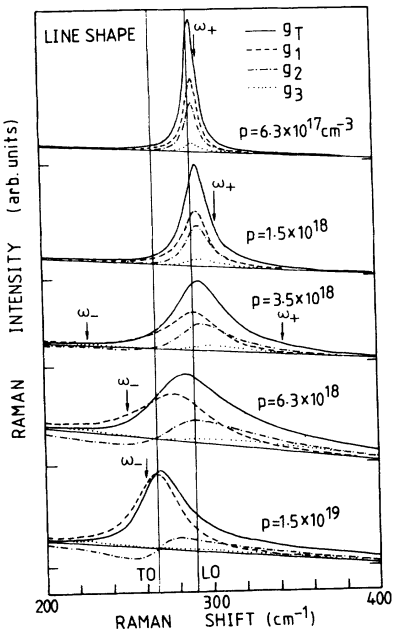

FIG. 5. Details of the Raman profile for different hole concentrations. g_T (solid lines) represent the observable line shapes, g_1 (broken lines), g_3 (dotted lines), and g_2 (dot-dashed lines) exhibit the line shapes due to atomic displacement fluctuations, macroscopic electric-field fluctuations, and their interference. The arrows denoted ω_+ and ω_- are the predicted frequencies of the coupled modes.

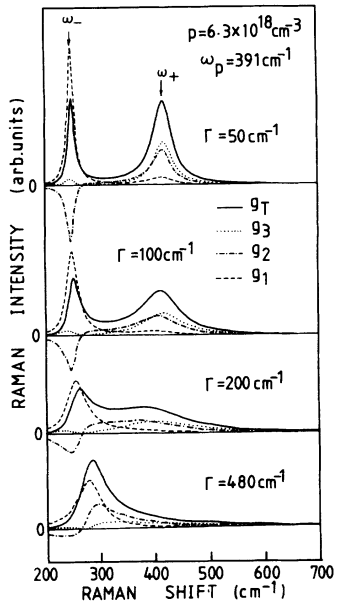

FIG. 6. Details of the Raman profile for four different values of Γ for $p=6.3\times10^{18}$ cm^{-3}. Symbols are the same as in Fig. 5.

cm^{-1}, and $\omega_+=418$ cm^{-1}. The calculated line shapes change drastically as Γ increases. For $\Gamma=50$ cm^{-1}, sharp Raman lines appear at ω_- and ω_+. The spectrum resembles that from n-type GaAs. But when the damping becomes heavy with $\Gamma=480$ cm$^{-1}>\omega_p=391$ cm^{-1}, the upper branch of the coupled LO-PL modes disappears, while the peak from the lower branch shifts to higher frequency with increased linewidth. This comes from dramatic changes in g_2 and the disappearance of g_3 with increased damping. From the results in Figs. 5 and 6, the asymmetric line shape for $p\geq3.5\times10^{18}$ cm^{-3} comes from interference between Raman scattering from atomic displacement fluctuations and from macroscopic electric-field fluctuations, modified by large plasmon damping. Our analysis also shows that the term $\mathrm{Im}(-1/\epsilon)$, sometimes used by itself to describe the line shape of the coupled modes in n-type GaAs,[3] is inadequate under conditions of large plasmon damping, for $\mathrm{Im}(-1/\epsilon)$ only describes the g_3 term.

As pointed out in Sec. I, disagreements about the behavior of the coupled LO-PL modes may come from the difficulty of combining the complex Raman profile from the bulk material with the profile due to the unscreened LO phonon in a surface depletion layer. We know of only one earlier relevant theoretical Raman analysis, that of Fukasawa *et al.*,[6] which uses a simple two-layer model[21] representing a surface depletion layer on a highly doped bulk semiconductor. For the Raman line-shape function, the analysis used the imaginary part of the classical response function of the atomic displacement $\langle\langle u(Q);u(Q')^*\rangle\rangle$. The inclusion of the surface layer, however, would have made the calculation intractable if we also used the full theory of Katayama and Murase with its interference effects. Instead we used the dispersive continuum model,[21,22] based on classical response theory,[23] to include correctly the unscreened LO phonon in the surface layer. [Its detailed expression has been given in Eqs. (10) and (11a)–(11d) of Ref. 6.] Although this omits the asymmetric features of the coupled-mode peaks, it gives a sufficiently good fit to justify the role of the surface layer in the Raman spectra.

We applied this theory to our present spectra, which cover a wider range of hole concentrations than in the earlier paper.[6] To calculate the line shape, we need the following material parameters: p, ω_{LO}, ω_{TO}, ϵ_∞, C, m_h^*, Γ, γ, the thickness of the surface depletion layer d_L, a constant v with dimensions of velocity, the scattering wave vector q, the absorption coefficient α, and the phonon damping constant in the surface depletion layer γ_1.

The values of ω_{LO}, ω_{TO}, ϵ_∞, C, m_h^*, v, q, and α for GaAs listed in Table I were fixed for all our calculations and the values of p, Γ, γ, and d_L were taken as listed in Table II. The values of p were determined from Hall measurements. If the bulk hole concentration p is equal to the density of ionized impurities N_i, d_L is estimated by $d_L=(\epsilon_0\phi/2\pi e^2N_i)^{1/2}$, where ϵ_0 and ϕ are the static dielectric constant and the barrier height of the surface potential for p-type GaAs, respectively.

Taking only γ_1 as an adjustable parameter, we fit the calculated Raman line shape to our data. Figure 7 shows the calculated and observed Raman spectra for all ten samples. Although there is only one adjustable parameter, the calculated line shapes agree well with the data for all ten samples. The fit values of γ_1 range from 5 to 9

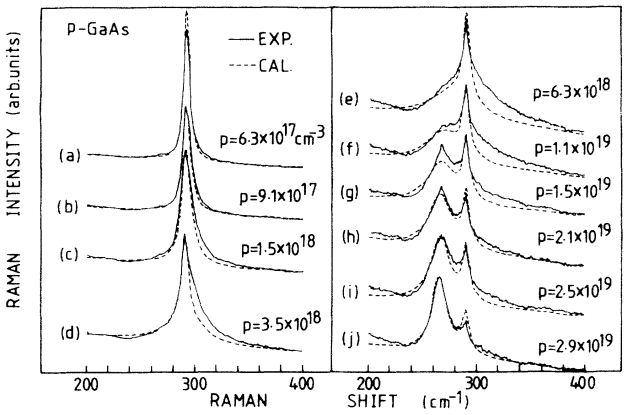

FIG. 7. Experimental (solid lines) and theoretical (broken lines) Raman spectra of the ten p-type GaAs samples. The broken lines represent Raman spectra calculated with the use of the theory of Raman scattering that includes surface depletion effects.

cm^{-1}, compared to a linewidth of 4.4 cm^{-1} for semi-insulating GaAs. The increase in γ_1 may arise from anharmonic effects due to the high-impurity doping. The simple two-layer model explains the systematic trends as a function of hole concentration, except for the discrepancy on the high-frequency side of the unscreened LO-phonon line for samples (d)–(f). Since the shoulder extending the high-frequency side originates from the g_2 term (see Fig. 5), the discrepancy comes because our simplified theory eliminates the interference between the atomic displacement and the electric-field fluctuations. The interference term is important in determining the asymmetric Raman line shape for samples (d)–(f).

IV. CONCLUSIONS

We have measured the room-temperature Raman spectra of ten Be-doped p-type GaAs samples with hole concentrations from 6.3×10^{17} to 2.9×10^{19} cm^{-3} and have observed single-mode behavior of the coupled LO-phonon–hole-plasmon modes in all of the samples. Furthermore, we performed a detailed line-shape analysis based on the theory of phonon Raman scattering due to the deformation-potential and electro-optic mechanisms. The theory reproduces the spectra fairly well for a wide range of hole concentrations and shows that the single-mode behavior of the coupled modes is due to the large damping of the hole plasmon. The analysis also reveals that the term g_3 associated with macroscopic electric-field fluctuations is negligibly small under conditions of large plasmon damping. This means that the upper and lower branches of the coupled modes in p-type GaAs are remarkably phononlike at all hole concentrations. Our analysis suggests that the character of the single mode changes from the damped upper branch to the damped lower branch with increasing hole concentration, which is quite different from the behavior of n-type GaAs. Finally, a theory of Raman scattering that includes surface depletion effects explains the line shape of the unscreened LO phonon. This indicates that the simple model of a surface depletion layer on a highly doped semiconductor is valid for a wide range of hole concentrations. To obtain more information about the plasmon damping constant of the LO-phonon–hole-plasmon system, we will continue to investigate the Raman spectra of these samples at low temperatures and will attempt to analyze our data with a full theory that includes both interference and surface layer effects.

ACKNOWLEDGMENTS

We would like to thank Dr. K. Ohta of the Electrotechnical Laboratory of the Ministry of International Trade and Industry for supplying and characterizing the samples. This work was supported in part by Emory University.

[1] I. Yokota, J. Phys. Soc. Jpn. **16**, 2075 (1961).
[2] B. Varga, Phys. Rev. **137**, A1896 (1965).
[3] G. Abstreiter, M. Cardona, and A. Pinczuk, in *Light Scattering in Solids IV*, edited by M. Cardona and G. Guntherodt (Springer-Verlag, Berlin, 1984).
[4] R. T. Holm, J. W. Gibson, and E. D. Palik, J. Appl. Phys. **48**, 212 (1977).
[5] R. Fukasawa, M. Wakaki, K. Ohta, and H. Okumura, Jpn. J. Appl. Phys. **25**, 652 (1986).
[6] R. Fukasawa, S. Katayama, A. Hasegawa, and K. Ohta, J. Phys. Soc. Jpn. **57**, 3632 (1988).
[7] T. Yuasa and M. Ishii, Phys. Rev. B **35**, 3962 (1987).
[8] K. Wan, J. F. Young, R. L. S. Devine, W. T. Moore, A. J. Spring Thorpe, C. J. Miner, and P. Mandeville, J. Appl. Phys. **63**, 5598 (1988).
[9] K. Wan and J. F. Young, Phys. Rev. B **41**, 10 772 (1990).
[10] S. Katayama and K. Murase, J. Phys. Soc. Jpn. **42**, 886 (1977).
[11] E. Burstein, A. Pinczuk, and S. Iwasa, Phys. Rev. **157**, 611 (1967).
[12] T. Sakamoto, H. Funabashi, K. Ohta, T. Nakagawa, N. J. Kawai, and T. Kojima, Jpn. J. Appl. Phys. **23**, L657 (1984).
[13] R. Loudon, Adv. Phys. **13**, 423 (1964).
[14] J. D. Wiley and M. DiDomenico, Jr., Phys. Rev. B **2**, 427 (1970).
[15] J. D. Wiley, in *Semiconductor and Semimetals*, edited by R. K. Willardson and A. C. Beer (Academic, New York, 1975), Vol. 10, p. 91.
[16] Q. H. F. Vrehen, J. Phys. Chem. Solids **29**, 129 (1968).
[17] R. Fukasawa, Y. Okubo, and K. Ohta, J. Spectrosc. Soc. Jpn. **40**, 215 (1991) [in Japanese].
[18] W. L. Faust and C. H. Henry, Phys. Rev. Lett. **17**, 1265 (1966).
[19] M. Gargouri, B. Prevot, and C. Schwab, J. Appl. Phys. **62**, 3902 (1987).
[20] A. Mlayah, R. Carles, G. Landa, E. Bedel, and A. Munoz-Yague, J. Appl. Phys. **69**, 4064 (1991).
[21] S. Katayama and R. Fukasawa, J. Phys. Soc. Jpn. **56**, 3726 (1987).
[22] M. Babiker, J. Phys. C **19**, 683 (1986).
[23] A. S. Barker and R. Loudon, Rev. Mod. Phys. **44**, 18 (1972).
[24] M. Haas and B. W. Henvis, J. Phys. Chem. Solids **23**, 1099 (1965).
[25] W. D. Johnston and I. P. Kaminow, Phys. Rev. **188**, 1209 (1969).
[26] W. G. Spitzer and C. A. Mead, J. Appl. Phys. **34**, 3061 (1963).